# Spectrally Enhancing Near-Field Radiative Transfer between Metallic Gratings by Exciting Magnetic Polaritons in Nanometric Vacuum Gaps

Yue Yang and Liping Wang

Phys. Rev. Lett. **117**, 044301 — Published 21 July 2016

DOI: 10.1103/PhysRevLett.117.044301

# Spectrally enhancing near-field radiative transfer between metallic gratings by exciting magnetic polariton in nanometric vacuum gaps

Yue Yang and Liping Wang*

*School for Engineering of Matter, Transport, and Energy*
*Arizona State University, Tempe, AZ, USA 85287*

* Corresponding author: *liping.wang@asu.edu*

**Abstract**

In the present work, we theoretically demonstrate that near-field radiative transport between one dimensional periodic grating microstructures separated by nanometer vacuum gaps can be spectrally enhanced by exciting magnetic polariton. Fluctuational electrodynamics that incorporates scattering matrix theory with rigorous coupled-wave analysis is employed to exactly calculate the near-field radiative flux between two metallic gratings. Besides the well-known coupled surface plasmon polaritons, the radiative flux can be also spectrally enhanced due to magnetic polariton, which is excited in the gap between grating ridges. The mechanisms of magnetic polariton in the near-field radiative transport are elucidated in detail, while the unusual enhancement cannot be predicted by either the Derjaguin's or effective medium approximations. The effects of vacuum gap distance and grating geometry parameters between the two gratings are investigated. The findings will open up a new way to spectrally control near-field radiative transfer by magnetic polariton with micro/nanostructured metamaterials, which holds great potential for improving the performance of energy systems like near-field thermophotovoltaic.

It has been demonstrated during the last decade that, radiative transfer could be significantly enhanced when distance between two objects is smaller than the characteristic thermal wavelength due to photon tunneling or coupling of evanescent waves [1-3]. In particular, near-field radiative flux could far exceed the blackbody limit by the resonant coupling of surface plasmon/phonon polaritons (SPP/SPhP) across the vacuum gap both theoretically and experimentally [4, 5]. Recently, excitations of magnetic SPhP [6, 7], hyperbolic modes [8-10], and epsilon-near-pole or epsilon-near-zero modes [11] with different types of metamaterials have also been studied to further improve the near-field radiative flux. Moreover, compared to the case of two plates, the near-field radiative transport between two gratings can be further enhanced due to guided modes [12] and spoof surface plasmon polaritons [13] between two Au gratings at a large vacuum gap distance of 1 μm, and hyperbolic modes between two doped silicon gratings [14]. Near-field thermal radiation could find many promising applications in energy-harvesting [1, 15], near-field imaging [16], and thermal management [17-22]. Several experimental methods have been reported to measure near-field radiative heat flux between planar surfaces at sub-micron vacuum gaps [23-25].

Magnetic polaritons (MP) refer to the strong coupling of external electromagnetic waves with the magnetic resonance excited inside the nanostructures. MP artificially realized with metallic micro/nanostructures have been employed to control light propagation and tailor exotic optical and radiative properties in the far field, such as selective solar absorber [26], thermophotovoltaic emitter [27], and switchable or tunable metamaterial [28, 29]. Phonon-mediated MP have also been excited in both SiC deep grating and binary grating configurations as well [30, 31]. On the other hand, the MP excitation has been achieved in the $SiO_2$ spacer between two Ag binary gratings [32]. In comparison to SPP/SPhP that has been well studied for tailoring both far- and near-field thermal radiation, magnetic resonance or MP has only been

investigated for controlling far-field thermal radiation while its role in near-field radiative transport has yet to be identified. In this work, we will theoretically investigate the possible effect of MP in near-field radiative transfer between two metallic grating microstructures separated by a vacuum gap $d$ below 100 nm.

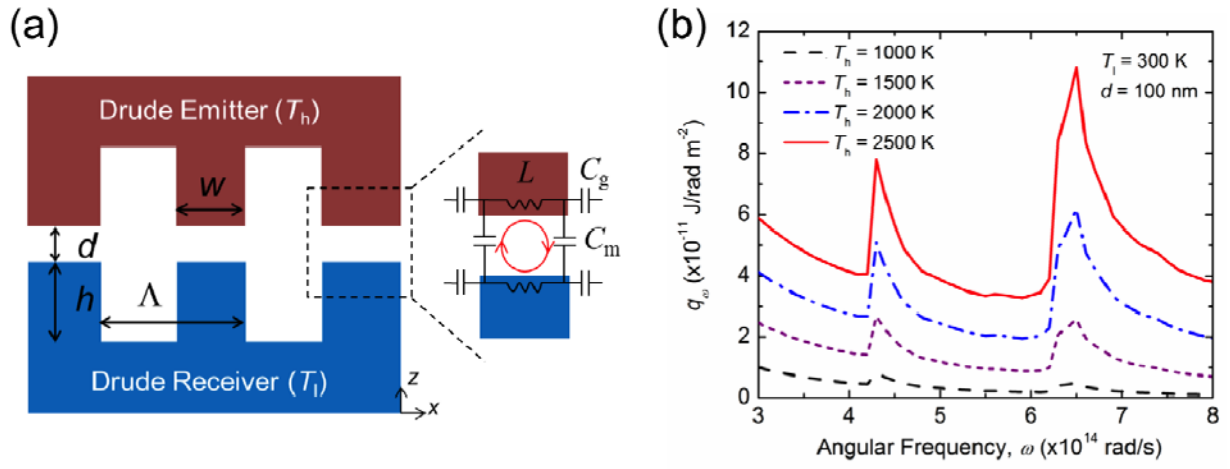


Fig. 1 (a) Schematic of radiative transfer between two symmetric, perfectly aligned metallic gratings with parameters of period ($\Lambda = 2$ μm), depth ($h$ = 1 μm), and ridge width ($w$ = 1 μm). The Drude emitter and receiver temperatures are respectively set as $T_h$ and $T_l$. The vacuum gap distance is denoted as $d$. An equivalent LC circuit model and the resulting electrical current loops in the vacuum gap at excitation of magnetic polariton (MP) are also depicted. (b) Spectral heat fluxes between these two perfectly aligned metallic gratings at different emitter temperatures when the receiver is separated by a vacuum gap of $d$ = 100 nm and maintained at $T_l$ = 300 K.

As depicted in Fig. 1(a), the gratings are assumed to be perfectly aligned with period, depth, and ridge width respectively as $\Lambda = 2$ μm, $h$ = 1 μm, and $w$ = 1 μm, which are kept unchanged in the present work unless specified. Vacuum is considered to be in the grating grooves, while the metal filling ratio is then $f = w/\Lambda = 0.5$. The temperatures of the emitter and receiver are set as $T_h$ and $T_l$, respectively. Note that an equivalent inductor-capacitor (LC) circuit model, which has been widely used to predict the MP resonance frequency in far field [32], is also shown in Fig. 1(a) along with the resulting current loop. The question is that whether MP resonance can be excited in the nanometer vacuum gap to spectrally enhance near-field radiative

transfer. To address this question, the scattering formalism [33-35] that is incorporated into fluctuational electrodynamics with rigorous coupled-wave analysis (RCWA) [36, 37] is employed to rigorously calculate the near-field radiative flux. The dielectric function of the metals is described by a Drude model as $\varepsilon_{\text{Drude}}(\omega)=1-\frac{\omega_p^2}{\omega^2+i\gamma\omega}$, where $\omega$ is the angular frequency, the plasma frequency is $\omega_p$ = $1.37\times10^{16}$ rad/s, and scattering rate is $\gamma$ = $7.31\times10^{13}$ rad/s [38], which are taken from the material properties of gold at room temperature as an example here. While the present study mainly focuses on the explanation of the physical mechanism and behavior of MP resonance in the near-field radiative transfer, similar MP excitation is expected to occur with other metals like Ag, Al, W [26, 27, 32], as well as some refractory plasmonic materials like ITO, AZO and TiN, which could possibly withstand high temperatures up to 3250 K [11].

Through the exact scattering theory, near-field spectral radiative transfer between two gratings is expressed as [39, 40]

$$q_\omega=\frac{1}{2\pi^3}\left[\Theta_{\text{h}}(\omega,T_{\text{h}})-\Theta_{\text{l}}(\omega,T_{\text{l}})\right]\int_0^{\pi/\Lambda}\int_0^{\infty}\xi(\omega,k_{x0},k_y)dk_y dk_{x0} \tag{1}$$

where $\Theta\left(\omega,T\right)=\hbar\omega/\left(e^{\hbar\omega/k_BT}-1\right)$ is the Planck oscillator, and $k_{x0}$ and $k_y$ are the incident wavevector components at the grating surface in the x and y directions, respectively. The energy transmission coefficient $\xi(\omega, k_{x0}, k_y)$, which considers all the polarization states, is

$$\xi\left(\omega,k_{x0},k_y\right)=\text{tr}\left(\mathbf{D}\mathbf{W}_1\mathbf{D}^\dagger\mathbf{W}_2\right) \tag{2a}$$

$$\mathbf{D}=\left(\mathbf{I}-\mathbf{S}_1\mathbf{S}_2\right)^{-1} \tag{2b}$$

$$\mathbf{W}_1=\Sigma_{-1}^{pw}-\mathbf{S}_1\Sigma_{-1}^{pw}\mathbf{S}_1^\dagger+\mathbf{S}_1\Sigma_{-1}^{ew}-\Sigma_{-1}^{ew}\mathbf{S}_1^\dagger \tag{2c}$$

$$\mathbf{W}_2=\Sigma_1^{pw}-\mathbf{S}_2^\dagger\Sigma_1^{pw}\mathbf{S}_2+\mathbf{S}_2^\dagger\Sigma_1^{ew}-\Sigma_1^{ew}\mathbf{S}_2 \tag{2d}$$

where **D** is the so-called Fabry-Perot denominator considering multiple reflection between two gratings, $\mathbf{W}_i$ indicate the photon absorption, $\mathbf{S}_1 = \mathbf{R}_1$, and $\mathbf{S}_2 = e^{ik_{z0}d}\mathbf{R}_2 e^{ik_{z0}d}$. $\mathbf{R}_1$ and $\mathbf{R}_2$ are the reflection operators of the two gratings, which can be obtained through RCWA method [36, 37, 41]. $k_x^{(n)} = k_{x0} + n\frac{2\pi}{\Lambda}$ is defined according to the Bloch wave condition. $n$ runs from $-N$ to $N$, where $N$ is the highest diffraction order. The operators $\Sigma_n^{pw/ew} = \frac{1}{2}k_z^n \Pi^{pw/ew}$, where $\Pi^{pw/ew}$ are the projectors on the propagative and evanescent sectors, were clearly defined in Ref. [39]. The details on the numerical convergence can be found in the Supplemental Materials, while our algorithm was validated by comparison with other works [12, 42] [See Figs. S1 and S2(a)]. The results obtained by the scattering matrix theory are treated to be rigorous.

Figure 1(b) presents the spectral heat fluxes between two metallic gratings at vacuum gap distance of $d$ = 100 nm with different emitter temperatures $T_h$ from 1000 K to 2500 K when the receiver temperature is fixed at $T_l$ = 300 K. There clearly exisit two spectral heat flux peaks around angular frequencies of $4.3\times10^{14}$ rad/s and $6.5\times10^{14}$ rad/s. As $T_h$ increases, the spectral peak locations surprisingly do not change, while the peak amplitudes are greatly enhanced mainly due to more energetic Planck oscillator at higher temperatures. For example, the spectral heat flux $q_\omega$ at the frequency of $6.5\times10^{14}$ rad/s could reach as high as $1.1\times10^{-10}$ J/rad m$^{-2}$ at $T_h$ = 2500 K. Note that, the angular frequency of $6.5\times10^{14}$ rad/s corresponds to 0.43 eV in energy, thus the observed spectral heat flux peaks could possibly greatly improve the thermophotovoltaic (TPV) energy conversion by spectrally enhancing photon transport above the bandgaps of TPV cells (e.g., $In_xGa_{1-x}As$ with band gaps varying from 0.36 eV to 1.42 eV).

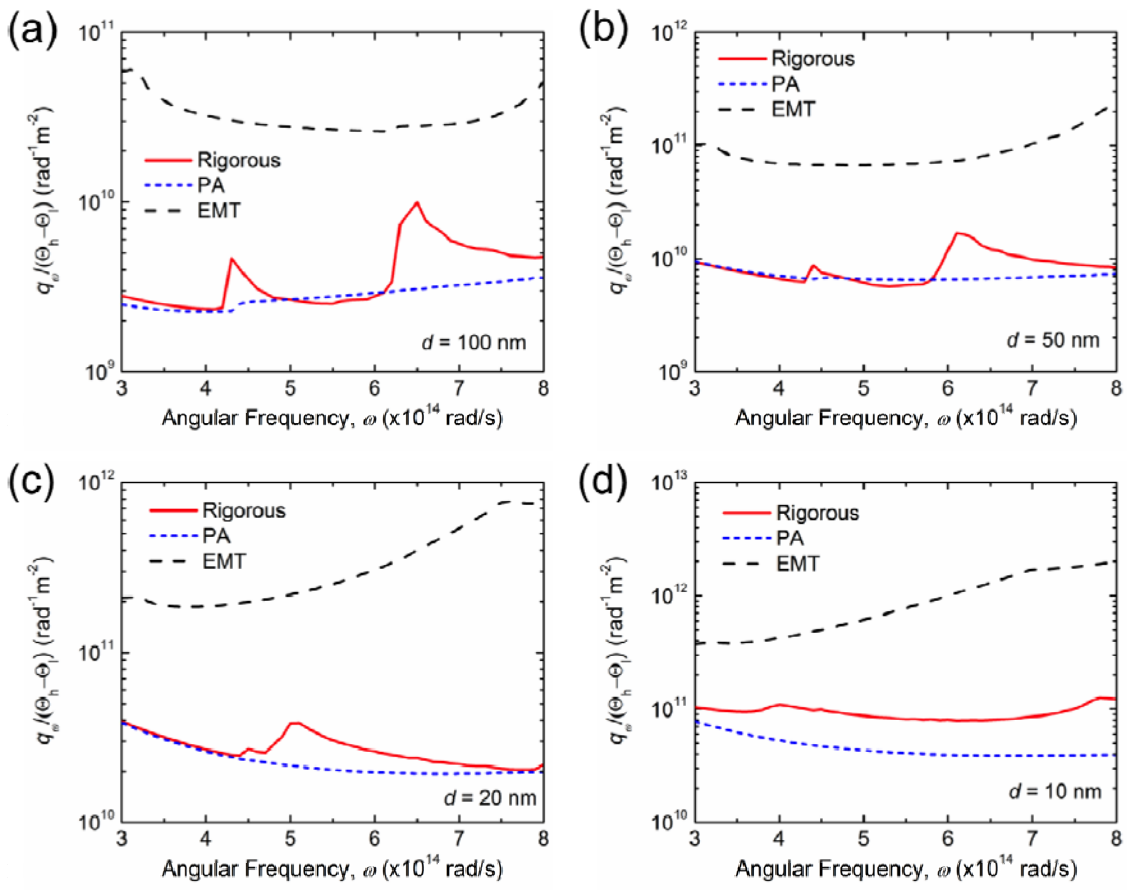


Fig. 2 Normalized spectral heat fluxes between the Drude grating emitter and receiver at different vacuum gaps of (a) $d$ = 100 nm, (b) $d$ = 50 nm, (c) $d$ = 20 nm, and (*d*) $d$ = 10 nm, obtained from the scattering matrix method (denoted as "Rigorous") in comparison with those from Derjaguin's proximity approximation method (denoted as "PA") and effective medium theory (denoted as "EMT").

In order to understand the physical mechanisms responsible for these two spectral heat flux peaks, we first investigate the spectral heat fluxes at different vacuum gap distances of $d$ = 100 nm, 50 nm, 20 nm and 10 nm as shown in Fig. 2. As the Planck oscillator only considers the effect of temperature, the spectral heat flux $q_\omega$ is normalized to the Planck oscillator difference $\Theta_h - \Theta_l$ in order to directly indicate the effects of materials and structures on the radiative transfer, which would better reveal the underlying mechanisms. It can be clearly observed from Fig. 2(a) that, at a vacuum gap distance of $d$ = 100 nm, there are two peaks of normalized

spectral heat flux at angular frequencies of $4.3\times10^{14}$ rad/s and $6.5\times10^{14}$ rad/s, respectively. When $d$ decreases to 50 nm the larger peak shifts to $\omega = 6.0\times10^{14}$ rad/s, and further to $5\times10^{14}$ rad/s at $d$ = 20 nm. However, when $d$ becomes 10 nm, there are two spectral peaks respectively at the frequencies of $4\times10^{14}$ rad/s and $7.8\times10^{14}$ rad/s, in addition to the small spectral peak around $\omega = 4.3\times10^{14}$ rad/s, whose frequency does not change at all at different vacuum gaps but the peak amplitude increases from $0.5\times10^{10}$ rad$^{-1}\cdot$m$^{-2}$ at $d$ = 100 nm to $1\times10^{11}$ rad$^{-1}\cdot$m$^{-2}$ at $d$ = 10 nm.

In order to understand the physical mechanisms responsible for the normalized spectral heat flux peaks predicted by the rigorous calculation, the Derjaguin's proximity approximation (PA) method, which represents a weighted approach for SPhP or SPP coupling with different vacuum gap distances, is first considered. The spectral heat flux between two gratings from the PA method can be weighted by the ones between two plates with different gap distances as

$$q_\omega^{\mathrm{PA}} = f \times q_\omega^{\mathrm{plate}}(d) + (1-f)\times q_\omega^{\mathrm{plate}}(d+2h) \tag{3}$$

where $q_\omega^{\mathrm{plate}}(L)$ means the spectral heat flux between two plates with a gap distance $L$. As inferred by Eq. (3), the PA method only considers the contributions by SPP coupling between planar surfaces at different vacuum gap distances. This indicates that the PA method would be accurate if coupled SPhP or SPP resonance is the only mechanism that dominates near-field radiative transfer [See Fig. S2 in the Supplemental Materials]. However, by comparing the normalized spectral heat flux from the PA method to the rigorous solution in Fig. 2, the PA method turns out to be accurate with good agreement with the rigorous solution except for the angular frequencies where spectral heat flux peaks exist for $d$ from 100 nm to 20 nm. At $d$ = 10 nm, the PA method fails to predict the exact values by significant discrepancies within the entire spectrum of interests. Apparently, the PA method or the SPP coupling between planar surfaces cannot explain the spectral heat flux peaks that exist between metallic gratings.

Furthermore, the effective medium theory (EMT), which considers the grating layer as a homogeneous uniaxial medium, is also examined on whether or not to be responsible for the spectral enhancement. By setting the diffraction order to zero in the RCWA algorithm, the metallic gratings are considered as effectively homogenous media with zero-order approximation [See Figs. S3 and S4 in the Supplemental Materials]. The near-field radiative flux between the metallic gratings with effective media approximation was also calculated and presented in Fig. 2 with different vacuum gaps. Comparing with the rigorous method, the EMT method overpredicts the normalized spectral heat flux by one order of magnitude, which is due to the enhancement from the hyperbolic modes unnecessarily predicted by the effective medium treatment [See the Supplemental Materials]. After all, EMT is inherently a homogenization approach which cannot take into account the local resonance modes like coupled SPP or MP that could possibly occur within the vacuum gap [14, 43, 44]. Therefore, effective medium approximation cannot explain the unusual radiative transfer between the metallic gratings across ultrasmall vacuum gaps, while physical mechanisms other than coupled SPP or EMT have to be identified and understood.

To gain a better idea on the radiative transfer between the Drude grating emitter and receiver, the contour plots of transmission coefficient in the $\omega$ - $k_{x0}$ domain under $k_y = 0$ from the rigorous method are presented in Fig. 3 at corresponding vacuum gap distances. Multiple bright horizontal bands, which are independent of $k_{x0}$ and indicate the enhanced near-field radiative transfer channels, can be clearly observed. Among different vacuum gap distances, the one at $\omega = 4.3\times10^{14}$ rad/s barely shifts with different d values, which is corresponding to the smaller spectral heat flux peak at the same frequency observed in Fig. 2. As intensively discussed in Ref. [12], this is associated with the guided mode, whose resonance condition strongly depends on the cavity depth, i.e. $H = 2h+d$. Note that the grating depth is $h = 1$ μm, which is much larger than the sub-100-nm vacuum gap distances considered here. Therefore, it can be understood that, the

guide mode would not shift when $d$ varies from 100 nm to 10 nm as $H \square d$. However, the same theory of guided modes cannot explain the brighter and broader resonance mode around $\omega$ = $6.5\times10^{14}$ rad/s at $d$ = 100 nm, which clearly shifts to lower frequencies with smaller $d$. As the coupled SPP, effective medium and guided modes cannot explain this particular unusual spectral enhancement between metallic gratings, could it be associated with possible excitation of magnetic resonance or MP?

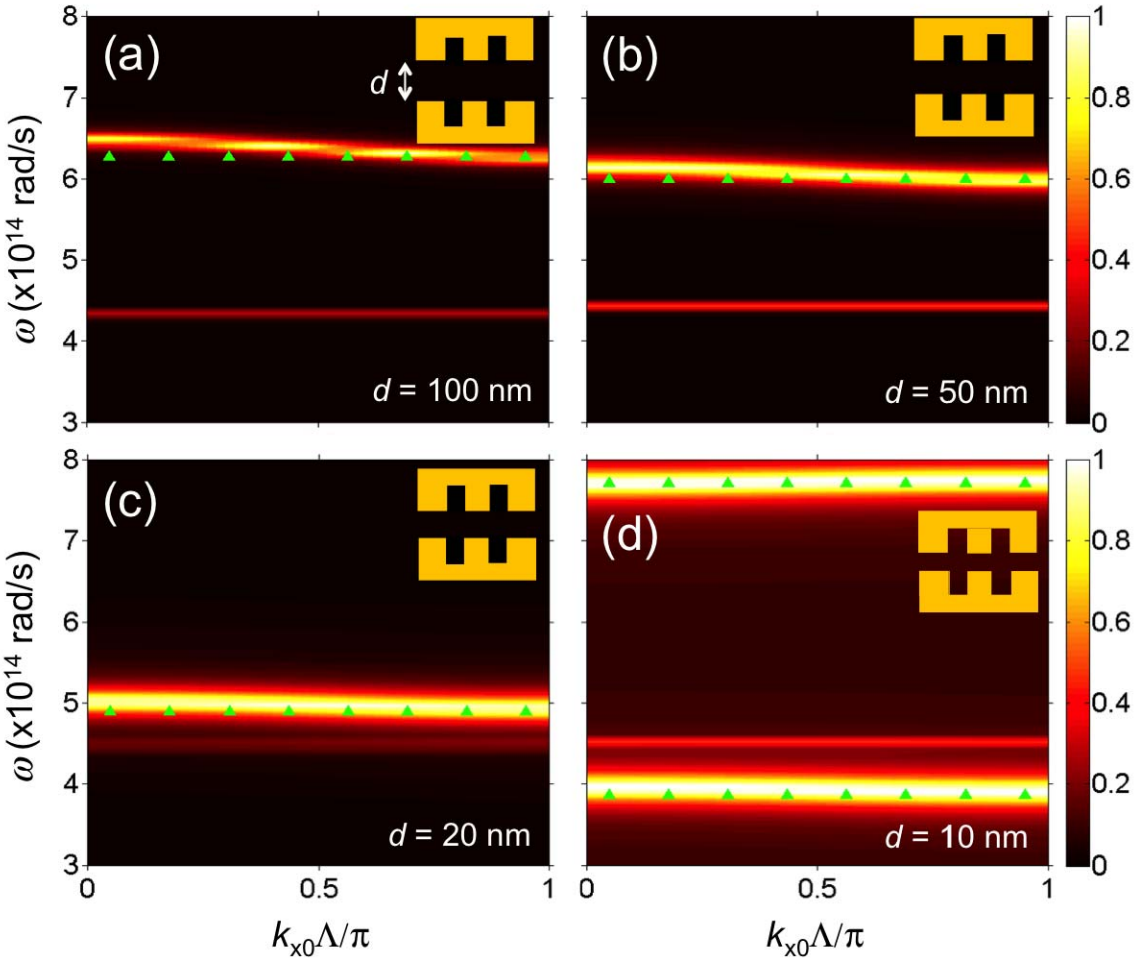


Fig. 3 Contour plots of energy transmission coefficient ($\xi$) between the Drude grating emitter and receiver at vacuum gaps of (a) $d$ = 100 nm, (b) $d$ = 50 nm, (c) $d$ = 20 nm, and (d) $d$ = 10 nm. The base geometric parameters of the metallic gratings are $\Lambda$ = 2 μm, $w$ = 1 μm, and $h$ = 1 μm. Note that $k_y$ = 0 is assumed and $k_{x0}$ is normalized to the first Brillouin zone. The LC circuit model prediction of MP resonance conditions is shown as green triangles.

In order to verify our hypothesis of MP resonance, an equivalent LC circuit is employed to analytically predict the resonance conditions of MP between two metallic gratings in near field [32]. Note that the LC model, based on the resonant charge distributions, has been successfully employed to verify the physical mechanisms of MP modes in metal-insulator-metal (MIM) nanostructures in selective control of far-field thermal radiation [29-32]. After all, the nanometer vacuum gap between the Drude grating emitter and receiver here forms similar MIM configurations [See Fig. S5 in the Supplemental Materials]. Here, the inductance of the metallic gratings can be expressed as $L = L_{\mathrm{m}} + L_{\mathrm{e}}$, where the first term $L_{\mathrm{m}} = 0.5\mu_0 wd$ accounts for the mutual inductance of two parallel plates with width $w$ separated by a distance $d$, and the kinetic inductance $L_{\mathrm{e}} = \omega/(\varepsilon_0 \omega_p^2 \delta)$ considers the contribution of drifting electrons. Note that $\mu_0$ and $\varepsilon_0$ are the permeability and permittivity of vacuum, while $\delta = \lambda/2\pi\kappa$ is the field penetration depth with $\kappa$ being the extinction coefficient of the metal. On the other hand, the parallel-plate capacitance between the upper and lower metal ridges can be expressed as $C_{\mathrm{m}} = c_1 \varepsilon_0 w/d$, where $c_1$ = 0.22 is the correction factor considering non-uniform charge distribution [32]. The capacitance between left and right metal ridges is denoted as $C_{\mathrm{g}} = \varepsilon_0 h/(\Lambda - w)$. Thus, the resonance frequency for the fundamental MP mode can be obtained when the total circuit impedance reaches zero:

$$\omega_{\mathrm{MP1}} = 1/\sqrt{(L_{\mathrm{m}} + L_{\mathrm{e}})(C_{\mathrm{m}} + C_{\mathrm{g}})} \tag{5}$$

With the base grating geometries as $\Lambda$ = 2 μm, $w$ = 1 μm, $h$ = 1 μm, the MP1 resonance frequencies between the Drude grating emitter and receiver are predicted to be $6.4\times10^{14}$ rad/s, $6.0\times10^{14}$ rad/s, $4.9\times10^{14}$ rad/s, and $3.8\times10^{14}$ rad/s respectively for $d$ = 100 nm, 50 nm, 20 nm, and 10 nm, which match surprisingly well with the unusual spectral enhancement mode predicted by the rigorous solution as shown in Fig. 3. Note that the independence of the MP

resonance condition on the $k_{x0}$ has been thoroughly discussed and well understood previously [31, 32]. At $d$ = 10 nm, the contour shows an additional resonance mode around $\omega = 7.7\times10^{14}$ rad/s, which is actually the second harmonic order of MP resonance with doubled resonance frequency from MP1. The unanimous agreements between the rigorous solution and the analytical LC model prediction at different vacuum gaps clearly verify the physical mechanism of MP excitation in spectrally enhancing near-field radiative transfer between metallic grating structures.

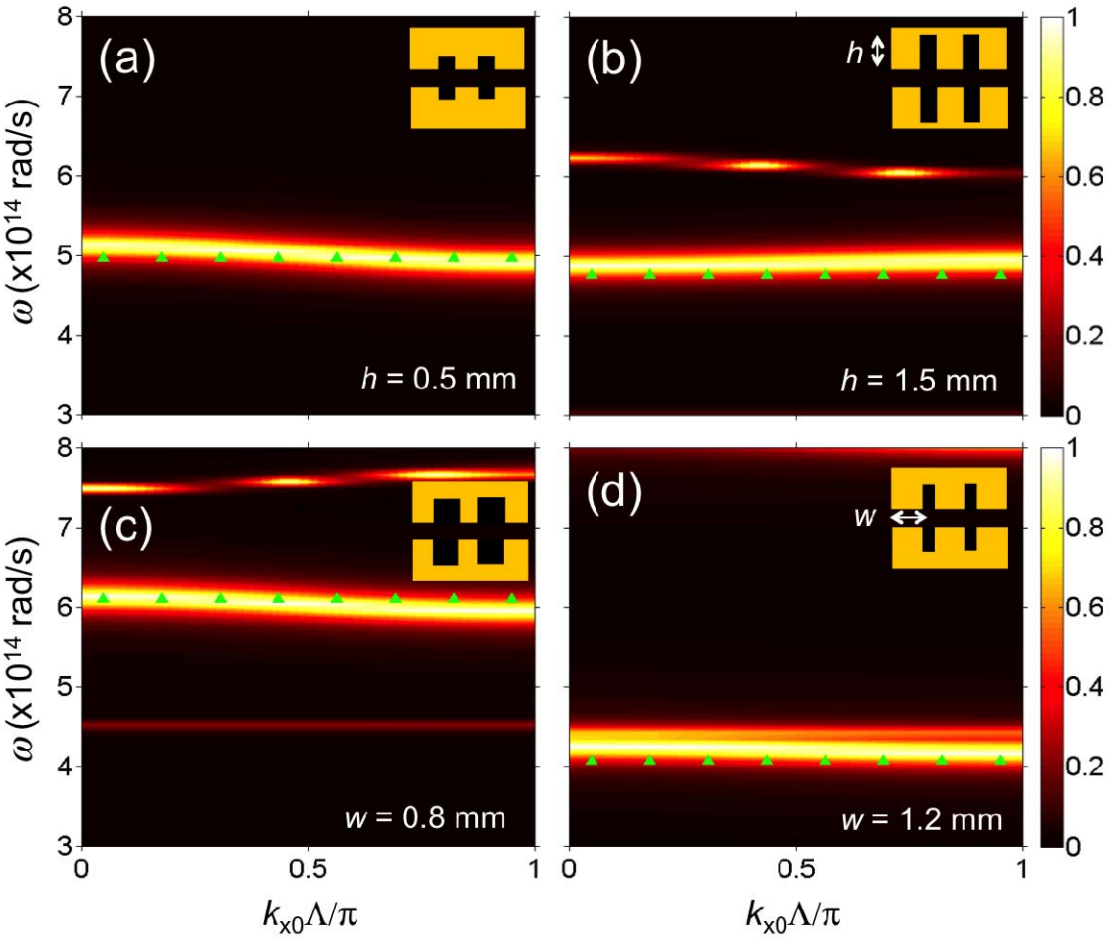


Fig. 4 Contour plots of energy transmission coefficient ($\xi$) between two perfectly aligned metallic gratings at $d$ = 20 nm with different geometries: (a) $h$ = 0.5 μm, (b) $h$ = 1.5 μm, (c) $w$ = 0.8 μm, and (d) $w$ = 1.2 μm, while the rest of parameters are kept at the base values: $\Lambda$ = 2 μm, $w$ = 1 μm, and $h$ = 1 μm. Note that $k_y$ = 0 is assumed and $k_{x0}$ is normalized to the first Brillouin zone. The LC circuit model prediction of MP resonance conditions is shown as green triangles.

To further confirm and understand the behaviors of MP resonance in near-field radiative transport across nanometer vacuum gaps, the grating geometric effect on near-field radiative transfer between the Drude grating emitter and receiver is investigated in terms of transmission coefficient at the gap distance $d$ = 20 nm. Figure 4(a) and 4(b) present the effect of grating depth respectively with $h$ = 0.5 μm and 1.5 μm, while other geometric parameters are kept at the base values. In comparison with the case of $h$ = 1 μm in Fig. 3(c), the strong and broad MP resonance mode around $\omega = 5\times10^{14}$ rad/s slightly shifts toward lower frequencies, which is in good agreement with the LC model prediction. Note that, the grating depth $h$ only affects the capacitance $C_g$, which is less than $C_m/10$ and thereby negligible with given parameters. Therefore, $h$ has little effect on the MP resonance condition. On the other hand, the guided mode, which strongly depends on the cavity depth, shifts from $4.3\times10^{14}$ rad/s to $6.2\times10^{14}$ rad/ when $h$ increases from 1 μm to 1.5 μm.

The effect of grating width ($w$) on the near-field radiative transfer spectrally enhanced by MP resonance is studied similarly in terms of transmission coefficient. By comparing Figs. 4(c) and 4(d) with 3(c), when the grating ridges becomes wider from 0.8 to 1.2 μm, both the rigorous solution and the LC model consistently show that the MP resonance mode changes from $\omega = 6.1\times10^{14}$ rad/s to $4.2\times10^{14}$ rad/s. From the perspective of charge distribution, grating width ($w$) is linear to $L_m$, $L_e$, and $C_m$. With negligible $C_g$ at $d$ = 20 nm, the MP resonance frequency $\omega_{MP1} \approx 1/\sqrt{(L_m + L_e)C_m}$ is essentially inversely proportional to $w$. Further tuning the geometric parameters of gratings, it is possible to shift the MP resonance and associated spectral flux peak to lower frequencies to better match the thermal wavelength at a given emitter temperature for total heat flux enhancement. On the contrary, the weaker guided mode around $\omega = 4.3\times10^{14}$ rad/s does not change with different grating width, whose resonance frequency is only a strong function of cavity depth H or grating depth $h$ [12]. Besides, the effect of grating misalignment

also confirms the consistent MP behaviors with different degrees of lateral displacement by the LC model [See Fig. S6 in the Supplemental Materials].

In summary, we have theoretically demonstrated unusual spectral radiative flux enhancement between two metallic grating emitter and receiver separated by sub-100-nm vacuum gaps, which neither SPP coupling, effective medium, nor guided mode could explain. The physical mechanisms have been identified and elaborated for the first time to be the excitation of magnetic polariton, unarguably verified by the consistency on the MP resonance modes between the rigorous solutions and the LC model predictions in terms of vacuum gap and geometric effects. The fundamental understanding gained here will open up a new way to spectrally tailor near-field radiative transfer with metamaterials for thermal management and energy harvesting applications.

**ACKNOWLEDGMENT**

This work was supported by the National Science Foundation under CBET-1454698.

## REFERENCES


[1] S. Basu, Z. M. Zhang, and C. J. Fu, Int. J. Energy Res. **33**, 1203 (2009).

[2] D. G. Cahill, P. V. Braun, G. Chen, D. R. Clarke, S. H. Fan, K. E. Goodson, P. Keblinski, W. P. King, G. D. Mahan, and A. Majumdar, Appl. Phys. Rev. **1**, 011305 (2014).

[3] D. G. Cahill, W. K. Ford, K. E. Goodson, G. D. Mahan, A. Majumdar, H. J. Maris, R. Merlin, and S. R. Phillpot, J. Appl. Phys. **93**, 793 (2003).

[4] J. Pendry, J. Phys. Condens. Matter **11**, 6621 (1999).

[5] S. Shen, A. Narayanaswamy, and G. Chen, Nano Lett. **9**, 2909 (2009).

[6] S. Basu and M. Francoeur, Appl. Phys. Lett. **99**, 143107 (2011).

[7] S. J. Petersen, S. Basu, and M. Francoeur, Photonics Nanostruct. **11**, 167 (2013).

[8] S.-A. Biehs, M. Tschikin, and P. Ben-Abdallah, Phys. Rev. Lett. **109**, 104301 (2012).

[9] C. Cortes, W. Newman, S. Molesky, and Z. Jacob, J. Opt. **14**, 063001 (2012).

[10] Y. Guo, C. L. Cortes, S. Molesky, and Z. Jacob, Appl. Phys. Lett. **101**, 131106 (2012).

[11] S. Molesky, C. J. Dewalt, and Z. Jacob, Opt. Express **21**, A96 (2013).

[12] R. Guérout, J. Lussange, F. S. S. Rosa, J.-P. Hugonin, D.A.R. Dalvit, J.-J. Greffet, A. Lambrecht and S. Reynaud, J. Phy. Conf. Ser. **395**, 012154 (2012).

[13] J. Dai, S. A. Dyakov and M. Yan, Phys. Rev. B **92**, 035419 (2015).

[14] X. L. Liu, B. Zhao and Z. M. Zhang, Phys. Rev. A **91**, 062510 (2015).

[15] K. Park, S. Basu, W. P. King, and Z. M. Zhang, J. Quant. Spectrosc. RA. **109**, 305 (2008).

[16] K. Hoshino, A. Gopal, M. S. Glaz, D. A. Vanden Bout, and X. Zhang, Appl. Phys. Lett. **101**, 043118 (2012).

[17] C. R. Otey, W. T. Lau, and S. Fan, Phys. Rev. Lett. **104**, 154301 (2010).

[18] L. P. Wang and Z. M. Zhang, Nanosc. Microsc. Therm. **17**, 337 (2013).

[19] Y. Yang, S. Basu, and L. P. Wang, Appl. Phys. Lett. **103**, 163101 (2013).

[20] P. Ben-Abdallah and S.-A. Biehs, Phys. Rev. Lett. **112**, 044301 (2014).

[21] Y. Yang, S. Basu, and L. P. Wang, J. Quant. Spectrosc. RA. **158**, 69 (2015).

[22] W. Gu, G. H. Tang and W. Q. Tao, Int. J. heat Mass Tran. **82**, 429 (2015).

[23] M. Lim, S. S. Lee, and B. J. Lee, Phys. Rev. B **91**, 195136 (2015).

[24] R. St-Gelais, B. Guha, L. Zhu, S. H. Fan, and M. Lipson, Nano Lett. **14**, 6971 (2014).

[25] K. Ito, A. Miura, H. Iizuka, and H. Toshiyoshi, Appl. Phys. Lett. **106**, 083504 (2015).

[26] H. Wang and L. Wang, Opt. Express **21**, A1078 (2013).

[27] B. Zhao, L. Wang, Y. Shuai, and Z. M. Zhang, Int. J. Heat Mass Tran. **67**, 637 (2013).

[28] H. Wang, Y. Yang, and L. Wang, Appl. Phys. Lett. **105**, 071907 (2014).

[29] H. Wang, Y. Yang and L. P. Wang, J. Appl. Phy. **116**, 123503 (2014).

[30] H. Wang, Y. Yang and L. P. Wang, J. Opt. **17**, 045104 (2015).

[31] L. P. Wang and Z. M. Zhang, Opt. Express **19**, A126 (2011).

[32] L. P. Wang and Z. M. Zhang, JOSA B **27**, 2595 (2010).

[33] G. Bimonte, Phys. Rev. A **80**, 042102 (2009).

[34] R. Messina and M. Antezza, Europhys. Lett. **95**, 61002 (2011).

[35] M. Krüger, T. Emig, and M. Kardar, Phys. Rev. Lett. **106**, 210404 (2011).

[36] L. Li, J. Opt. Soc. Am. A. **13**, 1870 (1996).

[37] M. G. Moharam, E. B. Grann, D. A. Pommet, and T. K. Gaylord, J. Opt. Soc. Am. A **12**, 1068 (1995).

[38] L. P. Wang, S. Basu and Z. M. Zhang, J. Heat Tran. **134**, 072701 (2012).

[39] A. Lambrecht and V. N. Marachevsky, Phys. Rev. Lett. **101**, 160403 (2008).

[40] J. Lussange, R. Guérout, F. S. S. Rosa, J.-J. Greffet, A. Lambrecht, and S. Reynaud, Phys. Rev. B **86**, 085432 (2012).

[41] R. Guérout, J. Lussange, H. B. Chan, A. Lambrecht and S. Reynaud, Phys. Rev. A **87**, 052514 (2013)

[42] X. L. Liu and Z. M. Zhang, Appl. Phys. Lett. **104**, 251911 (2014).

[43] H. Chalabi, E. Hasman and M. L. Brongersma, Phys. Rev. B **91**, 014302 (2015).

[44] X. L. Liu, T. J. Bright and Z. M. Zhang, J. Heat Tran. **136**, 092703 (2014).